

31. DeShazer, D., Wood, G. E. & Friedman, R. L. *BioTechniques* **17**, 288–289 (1994).  
 32. Border, C. J. *biof. Chem.* **256**, 1604–1607 (1981).  
 33. Wisden, W., Morris, B. J. & Hunt, S. P. in *Molecular Neurobiology: a Practical Approach* (eds Chad, J. & Wheal, H.), 205–225 (IRL/Oxford Univ. Press, Oxford, 1991).  
 34. Wilkinson, D. G. in *In situ Hybridization: a Practical Approach* (ed Wilkinson, D. G.) 75–83 (IRL/Oxford Univ. Press, Oxford, 1992).  
 35. Wilkinson, D. G. & Nieto, M. A. *Meth. Enzym.* **225**, 361–373 (1993).

ACKNOWLEDGEMENTS. We thank S. Offermanns and G. Schultz for GTP photoaffinity labelling, A. Schimmel, E. Bjørge, U. Ruffer (BASF) and A. Bach (BASF) for help with cloning and sequencing, A. Leyte and F. A. Barr for participating in preliminary experiments, P. Schrotz for advice on *in situ* hybridization, G. Schultz and K. Spicher as well as T. Pfeuffer and S. Moliner for antibodies and peptides, R. Edwards for the cDNA library, P. Argos, T. Etzold, M. Saraste and A. Wittinghofer for their helpful comments on the XLZs sequence, P. Gierschik, T. Pfeuffer and G. Schultz as well as our colleagues A. Schmidt and M. Ohashi for many helpful discussions, R. Bauerfeind, M. Hannah and M. Ohashi for comments on the manuscript and A. Summerfield for artwork. W.B.H. was supported by the SFB 317 of the Deutsche Forschungsgemeinschaft.

## Localization of pre-mRNA splicing in mammalian nuclei

Guohong Zhang\*, Krishan L. Taneja†, Robert H. Singer† & Michael R. Green\*

\* Howard Hughes Medical Institute, Program in Molecular Medicine, and † Department of Cell Biology, University of Massachusetts Medical Center, 373 Plantation Street, Worcester, Massachusetts 01605, USA

**In mammalian nuclei, precursor messenger RNA splicing factors are distributed non-uniformly. Antibodies directed against structural polypeptides of small nuclear ribonucleoprotein particles (snRNPs)<sup>1</sup> and some non-snRNP splicing factors<sup>2</sup> have shown that these components are concentrated in about 20–50 nuclear ‘speckles’. These and other non-homogeneous distributions have been proposed to indicate nuclear ‘compartments’ that are distinct from the sites of transcription and in which RNA processing occurs<sup>3–9</sup>. We have tested this idea using a new approach. Previous**

**structural<sup>10–13</sup> and biochemical<sup>14–16</sup> data have shown that splicing can occur in association with transcription. Nascent RNA of specific genes can be detected by *in situ* hybridization as intense spots of nuclear stain which map to the sites of transcription<sup>17–19</sup>. Here we identify active pre-mRNA splicing sites by localizing the nascent spliced mRNA of specific genes. We find that splicing occurs at the sites of transcription, which are not coincident with intranuclear speckles. We conclude that the nucleus is not compartmentalized with respect to transcription and pre-mRNA splicing.**

Initially, we analysed the well-characterized adenovirus type 2 (Ad2) major late pre-mRNA. HeLa cells were infected with Ad2, giving rise to a collection of identical, randomly distributed transcription units. Viral nucleic acids were localized by one-step *in situ* hybridization using fluorochrome-labelled oligonucleotide probes that were complementary to an untranscribed region of Ad2 DNA (DNA probe), an Ad2 intron (intron probe) or a splice-junction<sup>20</sup> (splice-junction probe) (Fig. 1, bottom; see legend for details). To avoid detecting signals of replicating viral DNA, Ad2-infected HeLa cells were treated with the DNA-synthesis inhibitor cytosine  $\beta$ -D-arabino-furanoside.

Figure 1 examines by digital imaging microscopy the collection of intranuclear signals obtained using the Ad2 DNA probe (Fig. 1a), intron probe (Fig. 1b), or splice-junction probe (Fig. 1c). Each of the probes gave rise to a similar pattern of about twenty intranuclear punctate signals. The signals were specific for Ad2 nucleic acids because no hybridization signals were observed in uninfected HeLa cells (d–f). The additional control experiments in Fig. 1 (g–l) demonstrate that the DNA, intron and splice-junction probes detected specifically Ad2 DNA, intron-containing Ad2 RNA and spliced Ad2 mRNA, respectively. Furthermore, all of the results in Figs 1 and 2 (see below) support the notion that each signal represents an Ad2 major late transcription unit.

To define the spatial relationship between transcription and splicing, we used pairwise combinations of the three probes using two-colour fluorophores (green and red). Cells were examined by digital imaging microscopy, allowing the images to be over-

FIG. 1 *In situ* detection of Ad2 nucleic acids in virally infected cells. *In situ* hybridization was used to detect Ad2 nucleic acids in HeLa cells using specific probes for DNA (a, d, g, j), an intron (IN; b, e, h, k), a splice-junction (SJ; c, f, i), or a splice-junction control probe (SJ-C, l). Cells were treated with 100  $\mu\text{g ml}^{-1}$  RNase (j, h, k, l) or 5 U per 30  $\mu\text{l}$  DNase (g, k) before hybridization. A diagram of the probes is also shown: boxes, exons; lines, introns.

METHODS. Oligonucleotides containing amino-modified thymidine (Glen Research) were synthesized (Model 394, Applied Biosystems), purified (on a 10% polyacrylamide gel) and labelled with fluorescein isothiocyanate (FITC) (Molecular Probes) or CY3 (BRL) in 0.1 M  $\text{NaHCO}_3/\text{Na}_2\text{CO}_3$  (pH 9.0) overnight (100-fold excess), and further purified through a Sephadex-G50 column and a 10% polyacrylamide gel. Probes: Ad2 splice-junction probe, 5'-CTCAACCGCGAG/CCCAACAGCTGG-3', complementary to the splice-junction sequence of the major late transcription unit, first and second leaders (6,066–6,077/7,099–7,110); the SJ-C probe was complementary to nucleotides 7,099–7,110/6,066–6,077; Ad2 intron probe, 5'-TTGTCTTTCTGACCAGATGGACG-3', complementary to intron sequence of 6,192–6,215; two Ad2 DNA-specific probes, 5'-GTGTTCCGCCACTTGCAACATC-3' and 5'-AATACACTGCGCGTCAGCT-GACTA-3', complementary to non-transcribed 5' DNA regions (121–144, 448–471). *In situ* hybridization: HeLa cells grown on glass coverslips were infected with Ad2 for 1 h at 100–200 PFU per cell in cytosine  $\beta$ -D-arabino-furanoside (araC, 20  $\mu\text{g ml}^{-1}$ ), grown for 18–24 h, fixed (in 4% paraformaldehyde for 15 min) and stored (in 70% ethanol at 4 °C), rehydrated in PBS and 2  $\times$  SSC. 20  $\mu\text{l}$  hybridization solution (20 ng probes, 20% formamide, 2  $\times$  SSC, 10% dextran sulphate, 1% BSA, 10  $\mu\text{g tRNA}$ , 10  $\mu\text{g single-stranded DNA}$ ) was added onto each coverslip, sealed with parafilm, and incubated for 2 h at 37 °C. For DNA probes, hybridization pretreatment of cells was at 70 °C in 70% formamide and 2  $\times$  SSC for 2 min. Washing was for 15 min each in 2  $\times$  SSC/20% formamide, 1  $\times$  SSC/20% formamide, 1  $\times$  SSC, PBS. Cells were examined by digital imaging microscopy after mounting in glycerol (Fig. 2 legend).

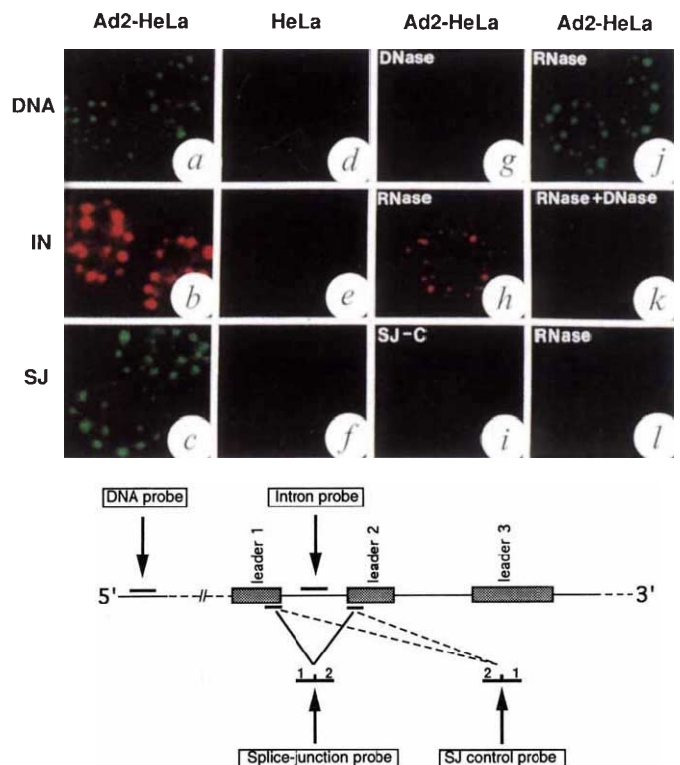
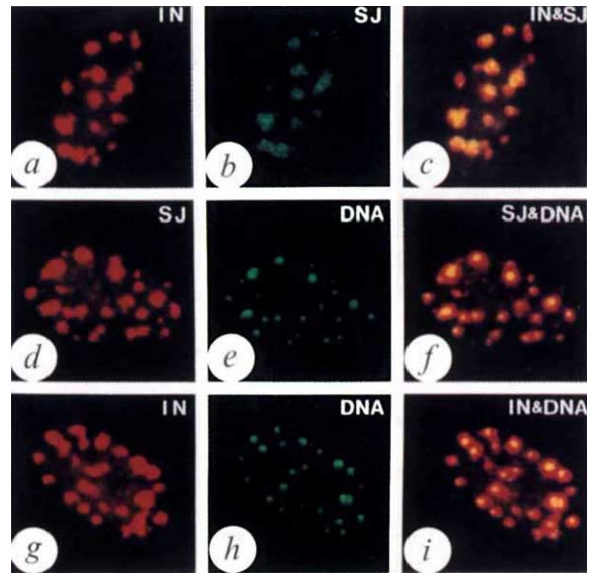


FIG. 2 Spatial relationship of Ad2 DNA and RNA signals. Spatial relationship of Ad2 spliced RNA, intronic RNA and Ad2 DNA examined by pairwise combinations using two-colour fluorophores: *a*, *b* and *c*, congruence of intronic Ad2 RNA (IN) relative to spliced Ad2 RNA (SJ); *d*, *e* and *f*, congruence of spliced Ad2 RNA (SJ) relative to Ad2 DNA (DNA); *g*, *h* and *i*, congruence of intronic Ad2 RNA relative to Ad2 DNA; *c*, *f* and *i*, alignment of green and red appears yellow.

METHODS. *In situ* hybridization is described in Fig. 1 legend. Images of cells were captured using a cooled charge-coupled device (CCD) camera, digitized and analysed<sup>30</sup>. Green and red pseudo-coloured images from the same optical plane were superimposed using dual-coloured fluorescence beads as fiducial markers.



laid with precise alignment. Alignment of the green and red signals results in yellow. Figure 2 shows that the signals detected with the DNA, intron and splice-junction probes co-localized, allowing several conclusions to be drawn. First, within the resolution of the light microscope, spliced Ad2 mRNA accumulated directly at the sites of Ad2 transcription. Second, the co-localization of the signals detected by the DNA and RNA probes indicates that no viral genome was located in a nuclear region that could not support transcription. Finally, the co-localization of the signals detected by the intron and splice-junction probes indicates that no viral transcription unit was located in a nuclear region that could not support splicing.

The spatial relationship of the Ad2 pre-mRNA splicing sites to the intranuclear speckles was visualized with the splice-junction probe (SJ in Fig. 3A). These same cells were stained by immunofluorescence using an anti-Sm antibody (Fig. 3A, *a-c*) which recognizes a component of snRNPs; an anti-3C5 antibody (Fig. 3A, *d-f*) which recognizes a family of conserved structural proteins present in the intranuclear speckles<sup>21</sup>; or an anti-SC35 antibody (Fig. 3A, *g-i*), which recognizes the essential splicing factor SC35<sup>2</sup>. With the anti-Sm and anti-3C5 antibodies, the sites of Ad2 pre-mRNA splicing appeared to be randomly distributed throughout the nucleoplasm and did not co-localize with intranuclear speckles (Fig. 3A, *c* and *f*). In contrast, the anti-SC35 antibody (Fig. 3A, *g-i*) indicated co-localization of Ad2 splicing sites with sites of concentrated SC35 (Fig. 3A, *i*).

To investigate why the results with the anti-SC35 antibody were anomalous, we compared the patterns detected with the three antibodies in uninfected and Ad2-infected HeLa cells. Figure 3B shows that in uninfected HeLa cells the signals detected by all three antibodies are co-localized. In contrast, following Ad2 infection (Fig. 3C), Sm and 3C5 antigen distributions are still co-localized (Fig. 3C, *g-i*), whereas the SC35 antigens no longer co-localized with Sm (Fig. 3C, *a-c*) and 3C5 (Fig. 3C, *d-f*) antigens.

We considered that the results with anti-SC35 antibody were due to cross-reaction with an Ad2 protein(s). Figure 3D shows that in an extract prepared from Ad2-infected cells, in addition to the expected SC35 band of  $M_r$  35,000 (35K; lane 1), a major 72K and a weaker 44K polypeptide were also detected (lane 2). Immunoblotting with an antibody directed against the Ad2 DNA-binding protein (DBP) demonstrated that the 72K and 44K polypeptides corresponded to intact Ad2 DBP and its C-

terminal proteolytic fragment<sup>22</sup> (DBP\*, lane 4). Consistent with this, Fig. 3E shows that in Ad2-infected cells SC35 co-localized with Ad2 DBP (Fig. 3E, *a-c*). As expected, DBP also co-localized with Ad2 DNA (Fig. 3E, *d-f*), the site of Ad2 transcription and splicing (Fig. 2). Thus, the apparent co-localization of SC35 and Ad2 splicing sites in Fig. 3A was due to cross-reaction of the anti-SC35 antibody with the Ad2 DBP (see also ref. 23).

Because our results were obtained with Ad2, an unintegrated viral genome, we analysed an endogenous cellular gene, the  $\beta$ -actin gene. Figure 4A shows that the  $\beta$ -actin-specific intron (Fig. 4A, *a*) or splice-junction (Fig. 4A, *b*) probe revealed two nuclear spots that co-localized (Fig. 4A, *c*). As expected, these RNA signals were coincident with the  $\beta$ -actin gene (data not shown). Figure 4B maps the  $\beta$ -actin signals detected with the splice-junction probe relative to the speckles. The results indicate that in most cases the nascent spliced  $\beta$ -actin RNA did not coincide with a nuclear speckle. In some cases, even within a single cell, one of the actively transcribed  $\beta$ -actin genes co-localized with a speckle whereas the other did not.

The spatial organization within the nucleus of pre-mRNA processing is controversial. We have shown that splicing of viral and cellular pre-mRNAs takes place spatially and temporally at the sites of these genes. There was only a random correlation between the sites of transcription and the nuclear speckled domains. Our results complement previous studies indicating that transcription occurs throughout the nucleus, with no evidence for compartmentalization<sup>24-26</sup>. Although our results show that different regions of the nucleus can support transcription and pre-mRNA splicing, we cannot yet exclude the speckles as processing sites for some pre-mRNAs.

In previous work, which also used adenovirus as a model, it was concluded that cellular splicing components move from the speckles to the sites of viral transcription<sup>27</sup>. In contrast, we find that the intranuclear distribution of speckles is unaffected by viral transcription, which occurs randomly throughout the nucleus. This discrepancy in our results may be explained as the previous work relied heavily upon the anti-SC35 antibody as a marker for speckles, which we have shown cross-reacts with Ad DBP (Fig. 3); also, inhibitors of viral DNA replication were not used<sup>27</sup>, and the resulting high levels of viral nucleic acids may have perturbed the normal distribution of cellular splicing factors.



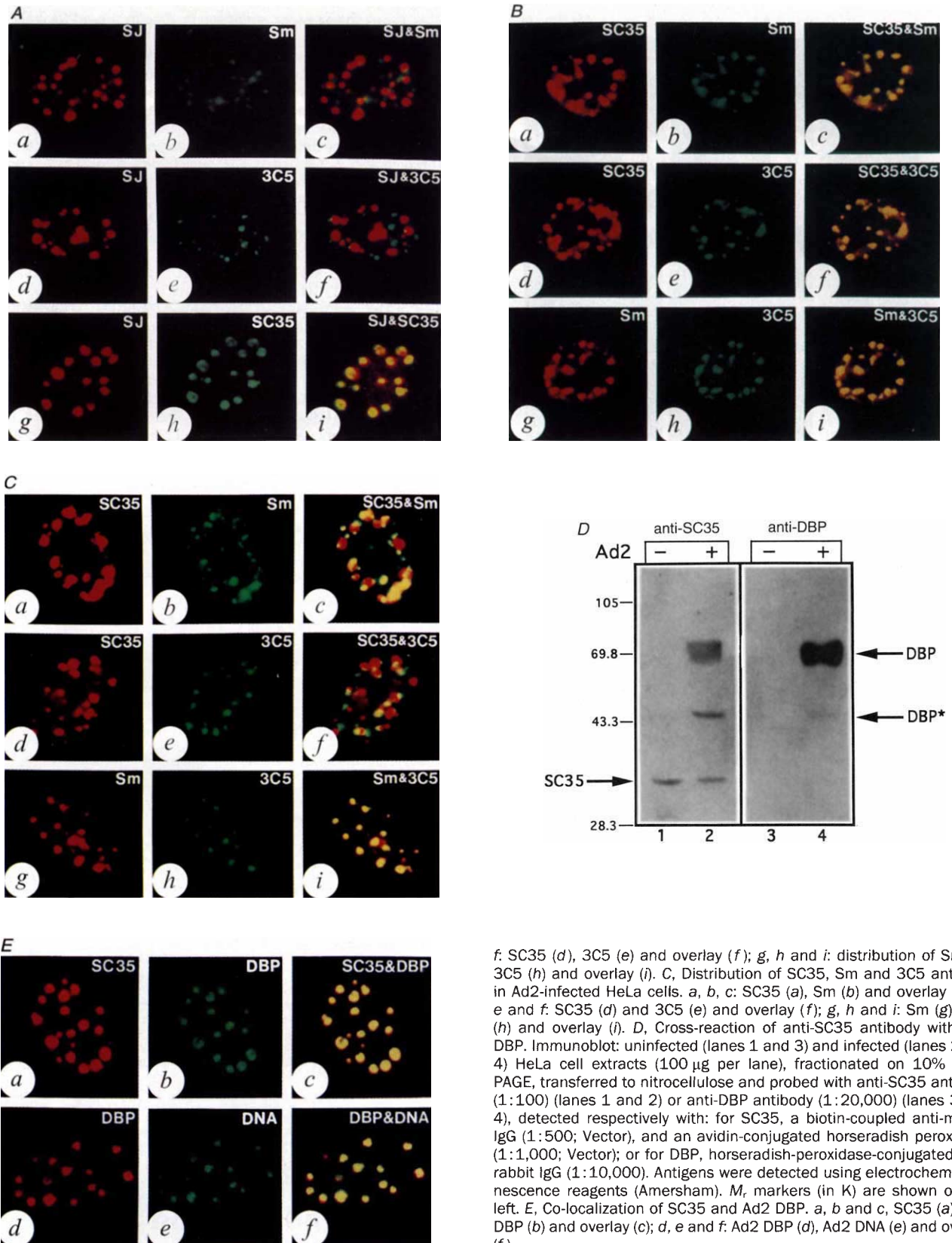


FIG. 3 Localizing sites of Ad2 pre-mRNA splicing. **A**, Spatial correlation of Ad2 splicing sites relative to intranuclear speckles. Distributions examined: *in situ* hybridization using the splice-junction probe (**a**, **d**, **g**) with immunofluorescence using anti-Sm (**b**), anti-3C5 (**e**) or anti-SC35 (**h**) antibodies. **B**, Distribution of SC35, Sm and 3C5 antigens in uninfected HeLa cells. **a**, **b** and **c**: SC35 (**a**), Sm (**b**) and overlay (**c**); **d**, **e** and **f**: SC35 (**d**) and 3C5 (**e**) and overlay (**f**); **g**, **h** and **i**: Sm (**g**), 3C5 (**h**) and overlay (**i**). **C**, Distribution of SC35, Sm and 3C5 antigens in Ad2-infected HeLa cells. **a**, **b**, **c**: SC35 (**a**), Sm (**b**) and overlay (**c**); **d**, **e** and **f**: SC35 (**d**) and 3C5 (**e**) and overlay (**f**); **g**, **h** and **i**: Sm (**g**), 3C5 (**h**) and overlay (**i**). **D**, Cross-reaction of anti-SC35 antibody with Ad2 DBP. Immunoblot: uninfected (lanes 1 and 3) and infected (lanes 2 and 4) HeLa cell extracts (100  $\mu$ g per lane), fractionated on 10% SDS-PAGE, transferred to nitrocellulose and probed with anti-SC35 antibody (1:100) (lanes 1 and 2) or anti-DBP antibody (1:20,000) (lanes 3 and 4), detected respectively with: for SC35, a biotin-coupled anti-mouse IgG (1:500; Vector), and an avidin-conjugated horseradish peroxidase (1:1,000; Vector); or for DBP, horseradish-peroxidase-conjugated anti-rabbit IgG (1:10,000). Antigens were detected using electrochemiluminescence reagents (Amersham). **M**, markers (in **K**) are shown on the left. **E**, Co-localization of SC35 and Ad2 DBP. **a**, **b** and **c**: SC35 (**a**), Ad2 DBP (**b**) and overlay (**c**); **d**, **e** and **f**: Ad2 DBP (**d**), Ad2 DNA (**e**) and overlay (**f**).

**METHODS.** After hybridization, cells were incubated with primary antibodies (PBS/1% BSA for 1 h), washed (PBS/0.1% BSA for 0.5 h), incubated with secondary antibodies (PBS/1% BSA for 1 h), rinsed and mounted onto glass slides. Antibody dilutions: anti-SC35 and anti-Sm antibodies, 1:100; anti-3C5 IgM, 1:4; anti-Sm (Immunovision), 1:40; FITC and CY3 (both Sigma) goat anti-mouse IgG secondary antibodies, 1:150 and 1:100, respectively; FITC goat anti-mouse IgM, 1:64; FITC goat anti-human IgG (Sigma), 1:40.

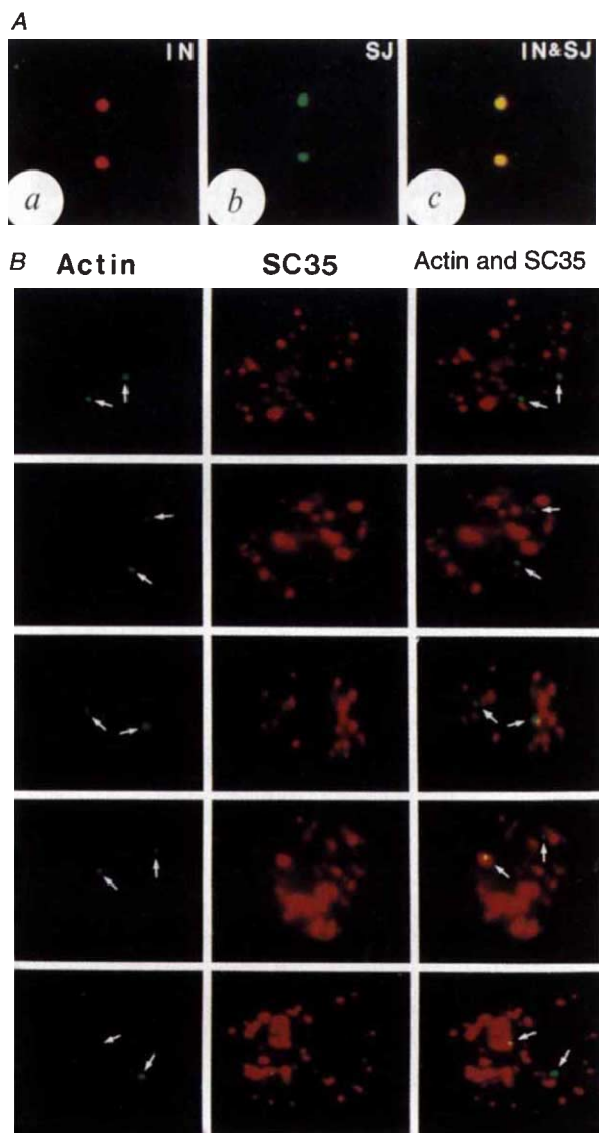


FIG. 4 Localizing sites of endogenous  $\beta$ -actin pre-mRNA splicing. **A**, Spatial correlation of unspliced and spliced  $\beta$ -actin RNAs. *In situ* hybridization signals detected using intron (a) and splice-junction (b) probes. (c), Overlay. **B**, Distribution of  $\beta$ -actin RNA relative to intranuclear speckles. Distributions of actively transcribed  $\beta$ -actin RNA (actin) relative to intranuclear speckles (SC35) in five representative cells. Nuclear  $\beta$ -actin RNA signals are indicated by arrows.

**METHODS.** Oligonucleotide probes contained 24 nucleotides complementary to actin sequence and 18 nucleotides of nonspecific sequence added to increase the fluorochromes. Intron-specific probes: IN1, 5'-GTCCCTGTGCGAGAAAGCGCCT-3'; IN2, 5'-CACGGCTAAGTGTGCTGGGGTCTT-3'; IN3, 5'-ATGAGGGCAGGACTTAGCTCCAC-3'; IN4, 5'-CTGACCTGCCAGGTCAGCTCAGG-3' complementary to the regions of 1,088–1,111, 1,744–1,768, 2,354–2,377 and 2,587–2,610. Splice-junction probes: SJ1, 5'-CACCATCACGCC/CTGGTGCCTGGG-3'; SJ2, 5'-CTCAAACATGAT/CTGGGTCATCTT-3'; SJ3, 5'-GGACTCCATGCC/CAGGAAGGAGG-3'; and SJ4, 5'-AGGAGCAATGAT/CTTGATCTTCAT-3' complementary to 1,028–1,039/1,074–1,085, 1,401–1,412/1,854–1,865, 2,281–2,292/2,388–2,399 and 2,559–2,570/2,683–2,694. Nonspecific sequences were: 5'-TTGCTTGCTTGCTTGCTT-3'. Morphometric analysis of nuclei was done on photographic images of optical sections from ten representative cells using a combined Image-Lab and Image-Measure program (Micro-Science, Inc.). The speckles occupied  $31 \pm 7\%$  of the nucleoplasmic area (excluding nucleoli). Of ten  $\beta$ -actin RNA signals, three coincided with nuclear speckles and one was in contact.

What then is the function of nuclear speckles? They could be sites for storage of splicing factors, or more simply sites where excess splicing factors accumulate, as indicated in a study of *Drosophila* polytene nuclei<sup>28</sup>. It has been shown in yeast that splicing factors are present in large functional excess<sup>29</sup>.

The approach described here can be extended to other genes in order to provide high spatial and temporal resolution of the transcription and processing of its pre-mRNA. The precise targeting of fluorochrome-labelled oligonucleotide probes to different regions of a large transcript, and the exact superimposition of these images by digital imaging microscopy, will allow a correlation of biochemical and structural events in the early life of an mRNA. □

13. Wu, Z., Murphy, C., Callan, H. G. & Gall, J. G. *J. Cell Biol.* **113**, 465–483 (1991).
14. Aebi, M. & Weissman, C. *Trends Genet.* **3**, 102–107 (1987).
15. LeMaire, M. F. & Thummel, C. S. *Molec. cell. Biol.* **10**, 6059–6063 (1990).
16. Baurén, G. & Wieslander, L. *Cell* **76**, 183–192 (1994).
17. O'Farrell, P. H., Edgar, B. A., Lakich, D. & Lehner, C. F. *Science* **246**, 635–640 (1989).
18. Shermoen, A. W. & O'Farrell, P. H. *Cell* **67**, 303–310 (1991).
19. Lawrence, J. B., Singer, R. H. & Marselle, L. M. *Cell* **57**, 493–502 (1989).
20. Valcarcel, J., Singh, R., Zamore, P. D. & Green, M. R. *Nature* **362**, 171–175 (1993).
21. Turner, B. M. & Franchi, L. *J. Cell Sci.* **87**, 269–282 (1987).
22. Voelkerding, K. & Klessig, D. F. *J. Virol.* **60**, 353–362 (1986).
23. Bridge, E., Carmo-Fonseca, M., Lamond, A. I. & Pettersson, U. *J. Virol.* **67**, 5792–5802 (1993).
24. Wansink, D. G. *et al. J. Cell Biol.* **122**, 283–293 (1993).
25. Jackson, D. A., Hassan, A. B., Errington, R. J. & Cook, P. R. *EMBO J.* **12**, 1059–1065 (1993).
26. Fakan, S., Leser, G. & Martin, T. E. *J. Cell Biol.* **98**, 358–363 (1984).
27. Jiménez-García, L. F. & Spector, D. L. *Cell* **73**, 47–59 (1993).
28. Zachar, Z., Kramer, J., Mims, I. P. & Bingham, P. M. *J. Cell Biol.* **121**, 729–742 (1993).
29. Séraphin, B. & Rosbash, M. *Cell* **59**, 349–358 (1989).
30. Taneja, K. L., Lifshitz, L. M., Fay, F. S. & Singer, R. H. *J. Cell Biol.* **119**, 1245–1260 (1992).

**ACKNOWLEDGEMENTS.** We thank B. M. Turner for anti-3C5, J. A. Steitz for anti-Sm, X. D. Fu for anti-3C5, and A. J. Levine and T. Linne for anti-DBP antibodies; A. Femino for help with detection of the  $\beta$ -actin RNA; X.-c. Zhu for flanking regions of the human  $\beta$ -actin gene; and R. Singh, J. Valcarcel and M. Zapp for comments on the manuscript. This work was made possible by the UMMC Biomedical Imaging Facility and was supported by NIH grants to M.R.G. and to R.H.S.

## ERRATUM

### Signal transduction and regulation in smooth muscle

Andrew P. Somlyo & Avril V. Somlyo

*Nature* **372**, 231–236 (1994)

IN the UK edition of *Nature*, Figs 1 and 2 of this Review Article were accidentally transposed during the production process. □

Received 22 July; accepted 10 November 1994.

1. Spector, D. L. *Proc. natn. Acad. Sci. U.S.A.* **87**, 147–151 (1990).
2. Fu, X. D. & Maniatis, T. *Nature* **343**, 437–441 (1990).
3. Spector, D. L. *A. Rev. Cell Biol.* **9**, 265–315 (1993).
4. Xing, Y. & Lawrence, J. B. *Trends Cell Biol.* **3**, 346–353 (1993).
5. Rosbash, M. & Singer, R. H. *Cell* **75**, 399–401 (1993).
6. Carter, K. C., Taneja, K. L. & Lawrence, J. B. *J. Cell Biol.* **115**, 1191–1202 (1991).
7. Spector, D. L., Fu, X. D. & Maniatis, T. *EMBO J.* **10**, 3467–3481 (1991).
8. Huang, S. & Spector, D. L. *Genes Dev.* **5**, 2288–2302 (1991).
9. Xing, Y., Johnson, C. V., Dobner, P. R. & Lawrence, J. B. *Science* **259**, 1326–1330 (1993).
10. Sass, H. & Pederson, T. *J. molec. Biol.* **180**, 911–926 (1984).
11. Beyer, A. L. & Osheim, Y. N. *Genes Dev.* **2**, 754–765 (1988).
12. Vazquez-Nin, G. H., Echeverría, O. M., Fakan, S., Leser, G. & Martin, T. E. *Chromosoma* **99**, 44–51 (1990).